

A novel (2+1)-dimensional complex coupled dispersionless system: Darboux transformation and multisolitons

H. W. A. Riaz and Ji Lin(林机)

Citation: Chin. Phys. B, 2025, 34 (**9**): 090502. DOI: 10.1088/1674-1056/adceff
http://cpb.iphy.ac.cn; http://iopscience.iop.org/cpb

What follows is a list of articles you may be interested in

Breather and its interaction with rogue wave of the coupled modified nonlinear Schrödinger equation

Ming Wang(王明), Tao Xu(徐涛), Guoliang He(何国亮), and Yu Tian(田雨)
Chin. Phys. B, 2023, 32 (**5**): 050503. DOI: 10.1088/1674-1056/ac833d

Dynamics of lump chains for the BKP equation describing propagation of nonlinear waves

Zhonglong Zhao(赵忠龙), Lingchao He(和玲超), and Abdul-Majid Wazwaz
Chin. Phys. B, 2023, 32 (**4**): 040501. DOI: 10.1088/1674-1056/acb0c1

Soliton molecules and dynamics of the smooth positon for the Gerdjikov–Ivanov equation

Xiangyu Yang(杨翔宇), Zhao Zhang(张钊), and Biao Li(李彪)†
Chin. Phys. B, 2020, 29 (**10**): 100501. DOI: 10.1088/1674-1056/ab9de0

Formation mechanism of asymmetric breather and rogue waves in pair-transition-coupled nonlinear Schrödinger equations

Zai-Dong Li(李再东), Yang-yang Wang(王洋洋), Peng-Bin He(贺鹏斌)
Chin. Phys. B, 2019, 28 (**1**): 010504. DOI: 10.1088/1674-1056/28/1/010504

Symmetry and asymmetry rogue waves in two-component coupled nonlinear Schrödinger equations

Zai-Dong Li(李再东), Cong-Zhe Huo(霍丛哲), Qiu-Yan Li(李秋艳), Peng-Bin He(贺鹏斌), Tian-Fu Xu(徐天赋)
Chin. Phys. B, 2018, 27 (**4**): 040505. DOI: 10.1088/1674-1056/27/4/040505

A novel (2+1)-dimensional complex coupled dispersionless system: Darboux transformation and multisolitons

H. W. A. Riaz[†] and Ji Lin(林机)[‡]

Department of Physics, Zhejiang Normal University, Jinhua 321004, *China*

(Received 12 March 2025; revised manuscript received 3 April 2025; accepted manuscript online 22 April 2025)

This study presents a (2+1)-dimensional complex coupled dispersionless system. A Lax pair is proposed, and the Darboux transformation is employed to construct multisoliton solutions. These solutions exhibit a range of wave phenomena, including bright and dark solitons, S-shaped formations, parabolic profiles, and periodic wave patterns. Additionally, it is shown that the system is equivalent to the sine-Gordon equation and the negative flow of the modified Korteweg–de Vries hierarchy through appropriate transformations.

Keywords: integrable systems, Darboux transformation, solitons

PACS: 05.45.Yv, 03.30.Kk, 02.30.Jr

DOI: 10.1088/1674-1056/adceff **CSTR:** 32038.14.CPB.adceff

1. Introduction

Nonlinear evolution equations play a crucial role in a variety of scientific disciplines, including fluid dynamics, condensed matter physics, and plasma physics.[1,2] These equations are notable for their integrability properties, which include the Lax pair structure, infinite conservation laws, and soliton solutions. The study of soliton equations has attracted significant attention, leading researchers to apply various mathematical techniques. Among these, scholars such as Ablowitz *et al.*,[3] Wang *et al.*,[4] Zhang *et al.*,[5] and Ma *et al.*[6] have thoroughly examined the inverse scattering method. Painlevé analysis has also received considerable attention, with contributions from Ablowitz *et al.*,[8] Liu *et al.*,[7] and Xu.[8] The Bäcklund transformation has been covered in works by Konno and Wadati,[9] Gao *et al.*,[10] and Xie and Fan.[11] The algebraic geometry approach received attention in work by Belokolos *et al.*,[12] while the authors in Ref. [13] explored the similarity reduction technique. Yao *et al.*[14] employed the bilinear method to investigate femtosecond soliton interactions influenced by higher-order nonlinear and dispersion effects. Similarly, Shao and Sudao in Ref. [15] used the method to derive and analyze localized and interaction solutions for a (3+1)-dimensional nonlinear equation. Among these methods, the Darboux transformation (DT) is thoroughly examined by Matveev and Salle.[16] This technique is well known for generating a variety of analytical solutions, including breather solutions,[17] as well as rational, periodic, bright, and dark solitons.[18] The generalized DT has been applied to the three-component Gross–Pitaevskii equations in $F = 1$ spinor Bose–Einstein condensates, leading to the derivation of high-order solutions, such as bright–dark–bright rogue waves, periodic waves, and their interactions.[19]

Over the past few decades, the dispersionless or quasiclassical limits of integrable equations and hierarchies have attracted significant interest from researchers. These limits emerge in the study of various problems in applied mathematics and physics, including quantum field theory and conformal mappings in the complex plane.[20,21] In Ref. [22], Konno and Ono introduced a coupled dispersionless (CD) integrable system, given by

$$\partial_\tau \rho + 2v\partial_\xi v = 0, \quad \partial_\xi \partial_\tau v - 2\rho v = 0, \tag{1}$$

where $\rho = \rho(\xi,\ \tau)$ and $v = v(\xi,\ \tau)$ are scalar functions of space and time, and ∂_τ and ∂_ξ represent partial derivatives with respect to the corresponding variables. The system equation (1) is referred to as dispersionless because it lacks a dispersion term, rather than arising as a semiclassical limit. A generalized form of the CD system, proposed by Kakuhata and Konno,[23] is expressed as

$$\begin{aligned} &\partial_\tau \rho + \partial_\xi (vw) = 0, \quad \partial_\xi \partial_\tau v - 2\rho v = 0, \\ &\partial_\xi \partial_\tau w - 2\rho w = 0, \end{aligned} \tag{2}$$

where $w = w(\xi,\tau)$ is a scalar function dependent on ξ and τ. When $w = v^*$, we obtain the complex CD system. Physically, the generalized CD system describes the interaction of a current-fed string in a specific external magnetic field.[24] The CD system and its complex counterpart have been shown to be gauge-equivalent to the sine-Gordon equation and the Pohlmeyer–Lund–Regge model.[24] More recently, the relationship between the motion of space curves, the real and complex CD systems, and the real and complex short-pulse equations has been established through hodograph transformations.[26] The CD and complex CD systems, along with their extensions to non-Abelian Lie groups and

[†]Corresponding author. E-mail: wajahat@zjnu.edu.cn

[‡]Corresponding author. E-mail: linji@zjnu.edu.cn

© 2025 Chinese Physical Society and IOP Publishing Ltd. All rights, including for text and data mining, AI training, and similar technologies, are reserved.

non-commutative versions, have been widely studied over the years. These systems can be fully solved using methods such as the Darboux transformation, Hirota's bilinear method, and other solution-generating techniques (see, for example, Refs. [26–28], and references therein).

A common approach in theoretical studies is to begin with the simplest models to grasp fundamental principles. In nonlinear physics, this often involves (1+1)-dimensional systems, where significant progress has been made. However, despite their simplicity, these systems remain an active area of research with many open questions. Moving to higher-dimensional systems is a natural step forward. Since the laws of nature are nonlinear and often modeled in multiple dimensions, studying higher-dimensional problems has become increasingly important. In this work, we focus on the complex CD (CCD) system in (2+1) dimensions, referred to as the (2+1)-CCD system hereafter, given by

$$\begin{aligned}&(\partial_\tau-\partial_\eta)\,\rho+\left(\partial_\xi-\partial_\eta\right)|v|^2=0,\\&\left(\partial_\xi-\partial_\eta\right)(\partial_\tau-\partial_\eta)\,v-2\rho v=0.\end{aligned}\tag{3}$$

Assuming that v is a real function, that is $v=v^*$, the system described by Eq. (3) is referred to as a real (2+1)-CD system. The solutions of the system (3) can be represented in terms of the solutions to the well-known equations.

(i) Using the transformations $\rho=(1/2)\cos u$ and $v=v^*=(1/2)(\partial_\tau-\partial_\eta)u$, where $u=u(\xi,\eta,\tau)$ is a real scalar function, the (2+1)-CCD system (3) reduces to the (2+1)-dimensional sine-Gordon equation[29]

$$\left(\partial_\eta-\partial_\xi\right)(\partial_\eta-\partial_\tau)\,u=\sin u.\tag{4}$$

(ii) Using $\rho=\sqrt{c-(\partial_\xi u-\partial_\eta u)(\partial_\xi u^*-\partial_\eta u^*)}$, where c is a constant, we convert the system (3) into

$$\begin{aligned}&\left(\partial_\xi-\partial_\eta\right)(\partial_\tau-\partial_\eta)\,v\\&=2\sqrt{c-(\partial_\xi v-\partial_\eta v)(\partial_\xi v^*-\partial_\eta v^*)}v.\end{aligned}\tag{5}$$

This equation is just the negative flow of modified Korteweg–de Vries hierarchy in (2+1) dimensions.[30]

(iii) Under the transformation $\rho(\xi,\ \eta,\ \tau)=P(\kappa,\ t)$, $v(\xi,\ \eta,\ \tau)=W(\kappa,\ t)$, $u(\xi,\ \eta,\ \tau)=Q(\kappa,\ t)$, and $\xi+\eta+\tau=\sigma$, $\xi=\kappa$, $\tau=t$, $\eta=\eta(\sigma,\ \kappa,\ t)$, $\xi=\xi(\sigma,\ \kappa,\ t)$, $\tau=\tau(\sigma,\ \kappa,\ t)$, we have

$$\partial_\eta=\partial_\sigma,\quad \partial_\xi=\partial_\sigma+\partial_\kappa,\quad \partial_\tau=\partial_\sigma+\partial_t,\tag{6}$$

and equations (3)–(5) reduce to their respective (1+1)-dimensional forms with new fields P, Q, and W:

$$\partial_t P+\partial_\kappa|W|^2=0,\tag{7}$$

$$\partial_t\partial_\kappa W-2PW=0,\tag{8}$$

$$\partial_\kappa\partial_t Q=\sin Q,\tag{9}$$

$$\partial_t\partial_\kappa W=2\sqrt{c-\partial_\kappa|W|^2}W.\tag{10}$$

In this work, we study a (2+1)-dimensional complex coupled dispersionless system and show that it is equivalent to the sine-Gordon equation and the negative flow of the modified Korteweg–de Vries hierarchy through suitable transformations. We construct a Lax pair for this system, which allows us to generate multisoliton solutions using DT. These solutions are expressed as ratios of simple determinants and exhibit diverse structures, including bright and dark solitons, S-shaped formations, parabolic profiles, and periodic wave patterns.

The paper is structured as follows. Section 1 provides an overview of the CD system, highlights significant past findings, and introduces the system (3). Section 2 discusses the Lax pair and DT, and elaborates on the derivation of multisoliton solutions for the system (3). Section 3 is dedicated to the computation and analysis of one- and two-soliton solutions against a zero background using DT. The paper concludes with Section 4, which summarizes the main findings and proposes potential avenues for future research.

2. Lax pair and Darboux transformation

The Lax pair of (2+1)-CCD system is given by the following system of linear differential equations:

$$\partial_\xi\Phi=\partial_\eta\Phi+\zeta\mathcal{U}\Phi,\tag{11}$$

$$\partial_\tau\Phi=\partial_\eta\Phi+(\zeta^{-1}\Gamma+\mathcal{V})\Phi,\tag{12}$$

where $\Phi=\Phi(\xi,\ \eta,\ \tau;\zeta)$ is the eigenfunction, ζ is the spectral parameter, the matrices U, V, and G are given by

$$\begin{aligned}&\mathcal{U}=-\mathrm{i}\begin{pmatrix}\rho & (\partial_\xi-\partial_\eta)v\\(\partial_\xi-\partial_\eta)v^* & -\rho\end{pmatrix},\quad \mathcal{V}=\begin{pmatrix}0 & -v\\v^* & 0\end{pmatrix},\\&\Gamma=\begin{pmatrix}\mathrm{i}/2 & 0\\0 & -\mathrm{i}/2\end{pmatrix}.\end{aligned}\tag{13}$$

The compatibility condition of the Lax pair [Eqs. (11) and (12)] yields (2+1)-CCD system (3). We now proceed to derive the DT of the (2+1)-CCD system. We utilize a DT to derive solutions for both the Lax pair and the (2+1)-CCD system (3). We introduce a new solution $\Phi^{[1]}$ of the Lax pair Eqs. (11)–(12), which is linked to the original solution Φ through a 2×2 matrix $T(\xi,\ \eta,\ \tau;\ \zeta)$, referred to as the Darboux matrix. The one-fold DT for the solution of the Lax pair is expressed as

$$\Phi^{[1]}\equiv T(\xi,\ \eta,\ \tau;\ \zeta)\Phi=(\zeta^{-1}I-M)\Phi,\tag{14}$$

where I is 2×2 identity matrix, and M is a 2×2 auxiliary matrix that simplifies the system, enabling the Lax pair formulation to derive soliton solutions in terms of specific matrix solutions. The matrix M is expressed as $M=\theta Z^{-1}\theta^{-1}$, where Z is a diagonal matrix of eigenvalues, and θ represents the matrix solution of the Lax pair equations (11) and (12):

$$\theta_\xi=\theta_\eta+\mathcal{U}\theta Z,\tag{15}$$

$$\theta_\tau=\theta_\eta+\Gamma\theta Z^{-1}+\mathcal{V}\theta.\tag{16}$$

Quasideterminants have found applications in the study of integrable systems, particularly in constructing multisoliton

solutions. The quasideterminant $|Y|_{ij}$ is defined as an expansion around the element y_{ij}

$$|Y|_{ij} = \begin{vmatrix} Y^{ij} & l_j^i \\ p_i^j & \boxed{y_{ij}} \end{vmatrix} = y_{ij} - p_i^j \left(Y^{ij}\right)^{-1} l_j^i, \tag{17}$$

where p_i^j is the i-th row of Y excluding the j-th entry, l_j^i is the j-th column of Y excluding the i-th row, and $Y^{ij} \neq 0$ is the submatrix obtained by removing the i-th row and j-th column from Y. For further details, see Ref. [31].

Theorem 1 Suppose $(\theta_1, \theta_2, \ldots, \theta_k)$ represents particular matrix solutions of the Lax pair defined in Eqs. (15) and (16), which correspond to the eigenvalues $(Z_1, Z_2, \ldots, Z_k)$, respectively. By using properties of quasideterminants. the k-fold application of the DT can be expressed as

$$\mathcal{U}^{[k]} = \mathcal{U} + (\partial_\xi - \partial_\eta) \begin{vmatrix} F & \mathcal{E}^{(k)} \\ \widetilde{F} & \boxed{\mathrm{O}} \end{vmatrix}, \tag{18}$$

where $\mathcal{E}^{(k)} = \begin{pmatrix} O & O & \cdots & I \end{pmatrix}$ is a $2k \times 2$ matrix, I and O denoting the identity and zero matrices of sizes 2×2, respectively. The matrix $\widetilde{F} = \begin{pmatrix} \theta_1^{(k)} & \theta_2^{(k)} & \cdots & \theta_k^{(k)} \end{pmatrix}$, the $2 \times 2k$ matrix, and F is a $2k \times 2k$ matrix given by

$$F = \begin{pmatrix} \theta_1 & \theta_2 & \ldots & \theta_k \\ \theta_1^{(1)} & \theta_2^{(1)} & \ldots & \theta_k^{(1)} \\ \vdots & \vdots & \ddots & \vdots \\ \theta_1^{(k-1)} & \theta_2^{(k-1)} & \ldots & \theta_k^{(k-1)} \end{pmatrix},$$

where $\theta^{(1)} = \theta Z^{-1}$, and $\theta^{(k)} = \theta Z^{-k}$.

Note that representing the solution as a ratio of determinants is more practical from a computational point of view. Therefore, rather than using quasideterminants, we simplify the representation of the solution Eq. (18) by stating it as a ratio of simple determinants. Thus, we have the following theorem.

Theorem 2 Suppose $\Phi_n = (\chi_n, \psi_n)^{\mathrm{T}}$ $(1 \leq n \leq 2k)$ represent the eigenfunctions of the Lax pair Eqs. (11)–(12) evaluated at the eigenvalues ζ_n. Then, $\rho^{[k]}$ and $v^{[k]}$ with the seed solutions $\rho = \rho^{[0]}$ and $v^{[0]}$ satisfy Eq. (3) and represents a solution to the system when $\chi_{2k} = -\psi_{2k-1}^*$, $\psi_{2k} = \chi_{2k-1}^*$ and $\zeta_{2k} = \zeta_{2k-1}^*$

$$\rho^{[k]} = \rho^{[0]} + \mathrm{i}(\partial_\xi - \partial_\eta) \begin{vmatrix} \frac{1}{\widetilde{\theta}} & \begin{vmatrix} \chi_1 & \cdots & \chi_{2k} & 0 \\ \psi_1 & \cdots & \psi_{2k} & 0 \\ \vdots & & \vdots & \vdots \\ \chi_1^{(k-1)} & \cdots & \chi_{2k}^{(k-1)} & 1 \\ \psi_1^{(k-1)} & \cdots & \psi_{2k}^{(k-1)} & 0 \\ \chi_1^{(k)} & \cdots & \chi_{2k}^{(k)} & 0 \end{vmatrix} \end{vmatrix},$$

$$v^{[k]} = v^{[0]} + \mathrm{i} \begin{vmatrix} \frac{1}{\widetilde{\theta}} & \begin{vmatrix} \chi_1 & \cdots & \chi_{2k} & 0 \\ \psi_1 & \cdots & \psi_{2k} & 0 \\ \vdots & & \vdots & \vdots \\ \chi_1^{(k-1)} & \cdots & \chi_{2k}^{(k-1)} & 0 \\ \psi_1^{(k-1)} & \cdots & \psi_{2k}^{(k-1)} & 1 \\ \chi_1^{(k)} & \cdots & \chi_{2k}^{(k)} & 0 \end{vmatrix} \end{vmatrix}, \tag{19}$$

where

$$\widetilde{\theta} = \begin{vmatrix} \chi_1 & \cdots & \chi_{2k} \\ \psi_1 & \cdots & \psi_{2k} \\ \vdots & & \vdots \\ \chi_1^{(k-1)} & \cdots & \chi_{2k}^{(k-1)} \\ \psi_1^{(k-1)} & \cdots & \psi_{2k}^{(k-1)} \end{vmatrix}. \tag{20}$$

3. Explicit solutions

In this section, we apply the DT to the fields of the (2+1)-CCD system (3) to explicitly derive solutions, including bright and dark solitons, S-shaped structures, parabolic forms, and periodic solitons. These solutions are obtained using the DT expressions Eq. (19) by starting with a constant seed solution and appropriately adjusting the free parameters. To calculate explicit expressions for solution of one and two solitons, we take the seed solution as $\rho = \rho^{[0]} = a$, $v = v^{[0]} = 0$, where a is a constant. In this background, we obtain the solutions to the Lax pair Eqs. (11)–(12):

$$\chi_n = \exp\left[-\mathrm{i}a\zeta_n\xi + \frac{\mathrm{i}}{2\zeta_n}\tau + A_n f(\xi, \eta, \tau)\right], \tag{21}$$

$$\psi_n = \exp\left[\mathrm{i}a\,\zeta_n\xi - \frac{\mathrm{i}}{2\zeta_n}\tau + B_n g(\xi, \eta, \tau)\right]. \tag{22}$$

Here, A_n and B_n are constants. By substituting Eqs. (21)–(22) into Eq. (19), we derive the one-fold $(k = 1)$ solution of the (2+1)-CCD system (3) under reduction $\chi_2 = -\psi_1^*$, $\psi_2 = \chi_1^*$,$\zeta_2 = \zeta_1^*$, $A_1 = B_2$, and $A_2 = B_1$, with the following choices for the arbitrary functions $f(\xi, \eta, \tau)$ and $g(\xi, \eta, \tau)$:

(I) When $f(\xi, \eta, \tau) = g(\xi, \eta, \tau) = (\xi + \eta + \tau)$:

$$\rho^{[1]} = a + \frac{-2(\zeta_1 - \zeta_2)^2 a\, \mathrm{e}^{2\mu_1(B_1+B_2)}}{\zeta_1\zeta_2\left(\exp\left(\frac{2\mathrm{i}a\xi\zeta_1\zeta_2^2 + (-2\mathrm{i}\zeta_1^2 a\xi + 4B_2\mu_1\zeta_1 + \mathrm{i}\tau)\zeta_2 - \mathrm{i}\tau\zeta_1}{2\zeta_1\zeta_2}\right) + \exp\left(\frac{2\mathrm{i}a\xi\,\zeta_1^2\zeta_2 + (-2\mathrm{i}\zeta_2^2 a\xi + 4B_1\mu_1\zeta_2 + \mathrm{i}\tau)\zeta_1 - \mathrm{i}\tau\zeta_2}{2\zeta_1\zeta_2}\right)\right)^2},$$

$$v^{[1]} = \frac{\mathrm{i}\,(\zeta_1 - \zeta_2)\exp\left(\frac{-2\mathrm{i}a\xi\,\zeta_1^2\zeta_2 + \left(-2\mathrm{i}\zeta_2^2 a\xi + 2(B_2+B_1)\mu_1\zeta_2 + \mathrm{i}\tau\right)\zeta_1 + \mathrm{i}\tau\zeta_2}{2\zeta_2\zeta_1}\right)}{\zeta_2\zeta_1\left(\exp\left(\frac{2\mathrm{i}a\xi\,\zeta_1\zeta_2^2 + (-2\mathrm{i}\zeta_1^2 a\xi + 4B_2\mu_1\zeta_1 + \mathrm{i}\tau)\zeta_2 - \mathrm{i}\tau\zeta_1}{2\zeta_1\zeta_2}\right) + \exp\left(\frac{2\mathrm{i}a\xi\,\zeta_1^2\zeta_2 + (-2\mathrm{i}\zeta_2^2 a\xi + 4B_1\mu_1\zeta_2 + \mathrm{i}\tau)\zeta_1 - \mathrm{i}\tau\zeta_2}{2\zeta_1\zeta_2}\right)\right)}, \tag{23}$$

where $\mu_1=\xi+\eta+\tau$.

(II) When $f(\xi,\ \eta,\ \tau)=g(\xi,\ \eta,\ \tau)=(\xi+\eta+\tau)^2$:

$$\begin{aligned}\rho^{[1]}&=a+\frac{-2(\zeta_1-\zeta_2)^2a\mathrm{e}^{2\mu_2(B_1+B_2)}}{\zeta_1\zeta_2\left(\exp\left(\frac{-2\mathrm{i}a\xi\ \zeta_1^2\zeta_2+(2\mathrm{i}\zeta_2^2a\xi+4\mu_2^2B_2\zeta_2-\mathrm{i}\tau)\zeta_1+\mathrm{i}\tau\zeta_2}{2\zeta_1\zeta_2}\right)+\exp\left(\frac{2\mathrm{i}a\xi\ \zeta_1^2\zeta_2+(-2\mathrm{i}\zeta_2^2a\xi+4\mu_2^2B_1\zeta_2+\mathrm{i}\tau)\zeta_1-\mathrm{i}\tau\zeta_2}{2\zeta_1\zeta_2}\right)\right)^2},\\ v^{[1]}&=\frac{\mathrm{i}\,(\zeta_1-\zeta_2)\exp\left(\frac{-2\mathrm{i}a\xi\ \zeta_1^2\zeta_2+\left(-2\mathrm{i}\zeta_2^2a\xi+2(B_2+B_1)\mu_2\zeta_2+\mathrm{i}\tau\right)\zeta_1+\mathrm{i}\tau\zeta_2}{2\zeta_2\zeta_1}\right)}{\zeta_1\zeta_2\left(\exp\left(\frac{-2\mathrm{i}a\xi\ \zeta_1^2\zeta_2+(2\mathrm{i}\zeta_2^2a\xi+4\mu_2^2B_2\zeta_2-\mathrm{i}\tau)\zeta_1+\mathrm{i}\tau\zeta_2}{2\zeta_1\zeta_2}\right)+\exp\left(\frac{2\mathrm{i}a\xi\ \zeta_1^2\zeta_2+(-2\mathrm{i}\zeta_2^2a\xi+4\mu_2^2B_1\zeta_2+\mathrm{i}\tau)\zeta_1-\mathrm{i}\tau\zeta_2}{2\zeta_1\zeta_2}\right)\right)},\end{aligned}\tag{24}$$

where $\mu_2=(\xi+\eta+\tau)^2$.

(III) When $f(\xi,\ \eta,\ \tau)=g(\xi,\ \eta,\ \tau)=\sin(\xi+\eta+\tau)$:

$$\begin{aligned}\rho^{[1]}&=a+\frac{-2(\zeta_1-\zeta_2)^2a\mathrm{e}^{2\mu_3(B_1+B_2)}}{\zeta_1\zeta_2\left(\exp\left(\frac{4B_2\mu_3\zeta_1\zeta_2-2\mathrm{i}(a\xi\zeta_2\zeta_1+\frac{\tau}{2})(\zeta_1-\zeta_2)}{2\zeta_1\zeta_2}\right)+\exp\left(\frac{4B_1\mu_3\zeta_1\zeta_2+2\mathrm{i}(a\xi\zeta_2\zeta_1+\frac{\tau}{2})(\zeta_1-\zeta_2)}{2\zeta_1\zeta_2}\right)\right)^2},\\ v^{[1]}&=\frac{\mathrm{i}\,(\zeta_1-\zeta_2)\exp\left(\frac{-2\mathrm{i}a\xi\ \zeta_1^2\zeta_2+\left(-2\mathrm{i}\zeta_2^2a\xi+2(B_2+B_1)\mu_3\zeta_2+\mathrm{i}\tau\right)\zeta_1+\mathrm{i}\tau\zeta_2}{2\zeta_2\zeta_1}\right)}{\zeta_1\zeta_2\left(\exp\left(\frac{4B_2\mu_3\zeta_1\zeta_2-2\mathrm{i}(a\xi\zeta_2\zeta_1+\frac{\tau}{2})(\zeta_1-\zeta_2)}{2\zeta_1\zeta_2}\right)+\exp\left(\frac{4B_1\mu_3\zeta_1\zeta_2+2\mathrm{i}(a\xi\zeta_2\zeta_1+\frac{\tau}{2})(\zeta_1-\zeta_2)}{2\zeta_1\zeta_2}\right)\right)},\end{aligned}\tag{25}$$

where $\mu_3=\sin(\xi+\eta+\tau)$.

(IV) When $f(\xi,\ \eta,\ \tau)=g(\xi,\ \eta,\ \tau)=(\xi+\eta+\tau)^3$:

$$\begin{aligned}\rho^{[1]}&=a+\frac{-2(\zeta_1-\zeta_2)^2a\mathrm{e}^{2\mu_4(B_1+B_2)}}{\zeta_1\zeta_2\left(\exp\left(\frac{2\mathrm{i}ay\zeta_1\ \zeta_2^2+(-2\mathrm{i}\zeta_1^2ay+4B_2\mu_4^3\zeta_1+\mathrm{i}t)\zeta_2-\mathrm{i}t\zeta_1}{2\zeta_1\zeta_2}\right)+\exp\left(\frac{2\mathrm{i}ay\ \zeta_1^2\zeta_2+(-2\mathrm{i}\zeta_2^2ay+4\mu_4^3B_1\zeta_2+\mathrm{i}t)\zeta_1-\mathrm{i}t\zeta_2}{2\zeta_1\zeta_2}\right)\right)^2},\\ v^{[1]}&=\frac{\mathrm{i}\,(\zeta_1-\zeta_2)\exp\left(\frac{-2\mathrm{i}a\xi\ \zeta_1^2\zeta_2+\left(-2\mathrm{i}\zeta_2^2a\xi+2(B_2+B_1)\mu_4\zeta_2+\mathrm{i}\tau\right)\zeta_1+\mathrm{i}\tau\zeta_2}{2\zeta_2\zeta_1}\right)}{\zeta_1\zeta_2\left(\exp\left(\frac{2\mathrm{i}ay\zeta_1\ \zeta_2^2+(-2\mathrm{i}\zeta_1^2ay+4B_2\mu_4^3\zeta_1+\mathrm{i}t)\zeta_2-\mathrm{i}t\zeta_1}{2\zeta_1\zeta_2}\right)+\exp\left(\frac{2\mathrm{i}ay\zeta_1^2\zeta_2+(-2\mathrm{i}\zeta_2^2ay+4\mu_4^3B_1\zeta_2+\mathrm{i}t)\zeta_1-\mathrm{i}t\zeta_2}{2\zeta_1\zeta_2}\right)\right)},\end{aligned}\tag{26}$$

where $\mu_4=2(\xi+\eta+\tau)^3$.

In Eqs. (23)–(26), we derived the one-fold solution, which serves as a foundation for obtaining more general solutions of the (2+1)-CCD system (3). The solutions $\rho^{[1]}$ and $v^{[1]}$ in Eq. (23) correspond to dark and bright solitons, respectively, and solutions $\rho^{[1]}$ and $v^{[1]}$ in Eq. (24) correspond to dark and bright parabolic structures. Equation (25) describes periodic solitons, while equation (26) produces S-shaped soliton structures. Note that, when the function $f(\xi,\eta,\tau)=\xi+\eta+\tau$ is linear, the envelope soliton propagates with a well-defined velocity, given by

$$v_\eta=\frac{(B_1-B_2)(B_1-B_2-\zeta_{1\mathrm{I}}/|\zeta_1|^2)}{4(a^2\zeta_{1\mathrm{I}}^2-(B_1-B_2)a\zeta_{1\mathrm{I}}+(B_1-B_2)^2/2)}$$

in the η-direction and

$$v_\xi=\frac{(B_1-B_2-2a\zeta_{1\mathrm{I}})(B_1-B_2-\zeta_{1\mathrm{I}}/|\zeta_1|^2)}{4(a^2\zeta_{1\mathrm{I}}^2-(B_1-B_2)a\zeta_{1\mathrm{I}}+(B_1-B_2)^2/2)}$$

in the ξ-direction. However, when $f(\xi,\eta,\tau)$ is quadratic, sinusoidal, or cubic, the argument of the envelope function contains nonlinear terms, introducing spatial and temporal variations in velocity. As a result, the envelope no longer moves with a uniform speed, and the soliton may experience deformation, acceleration, or changes in its shape over time. The propagation dynamics become more intricate, depending on the form of $f(\xi,\eta,\tau)$. These solutions are plotted in Fig. 1.

Next, we compute the two-soliton solution using the two-fold ($k=2$) DT from Eq. (19). These solutions can be classified based on different behaviors observed in the $(2+1)$-dimensional system. Hence, we have

$$\begin{aligned}\rho^{[2]}&=\rho^{[0]}+\mathrm{i}(\partial_\xi-\partial_\eta)\left[\frac{1}{\widetilde{\theta}}\begin{vmatrix}\chi_1&\cdots&\chi_4&0\\ \psi_1&\cdots&\psi_4&0\\ \chi_1^{(1)}&\cdots&\chi_4^{(1)}&1\\ \psi_1^{(1)}&\cdots&\psi_4^{(1)}&0\\ \chi_1^{(2)}&\cdots&\chi_4^{(2)}&0\end{vmatrix}\right],\\ v^{[2]}&=v^{[0]}+\mathrm{i}\left[\frac{1}{\widetilde{\theta}}\begin{vmatrix}\chi_1&\cdots&\chi_4&0\\ \psi_1&\cdots&\psi_4&0\\ \chi_1^{(1)}&\cdots&\chi_4^{(1)}&0\\ \psi_1^{(1)}&\cdots&\psi_4^{(1)}&1\\ \chi_1^{(2)}&\cdots&\chi_4^{(2)}&0\end{vmatrix}\right],\end{aligned}\tag{27}$$

where

$$\widetilde{\theta}=\begin{vmatrix}\chi_1&\cdots&\chi_4\\ \psi_1&\cdots&\psi_4\\ \chi_1^{(1)}&\cdots&\chi_4^{(1)}\\ \psi_1^{(1)}&\cdots&\psi_4^{(1)}\end{vmatrix},\quad \chi_1^{(1)}=\zeta_1^{-1}\chi_1,\ \psi_1^{(1)}=\zeta_1^{-1}\psi_1.\tag{28}$$

By solving Eq. (27) using symbolic computation, we have

$$\rho^{[2]} = a + \mathrm{i}(\partial_\xi - \partial_\eta)\frac{\rho_{\mathrm{num}}}{d_1}, \quad v^{[2]} = \frac{v_{\mathrm{num}}}{d_1}, \tag{29}$$

where ρ_{num}, v_{num}, and d_1 are respectively given in Eqs. (A1)–(A3) in Appendix A.

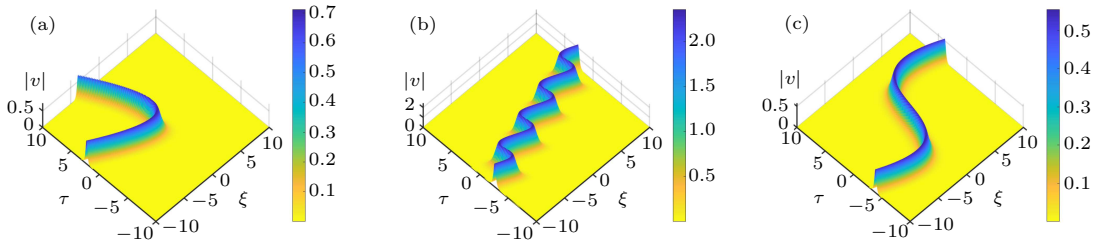


Fig. 1. Profiles of the solutions from Eqs. (24)–(26), under different parameter configurations: (a) corresponds to solution Eq. (24) with $\zeta_{1\mathrm{R}} = 0.1$, $\zeta_{1\mathrm{I}} = 1.4$, and $B_1 = -B_2 = 0.2$; (b) corresponds to solution Eq. (25) with $\zeta_{1\mathrm{R}} = 0.1$, $\zeta_{1\mathrm{I}} = 0.4$, and $B_1 = -B_2 = -1.5$; (c) corresponds to solution Eq. (26) $\zeta_{1\mathrm{R}} = -0.1$, $\zeta_{1\mathrm{I}} = 1.8$, and $B_1 = -B_2 = -0.005$, and $a = -0.8$.

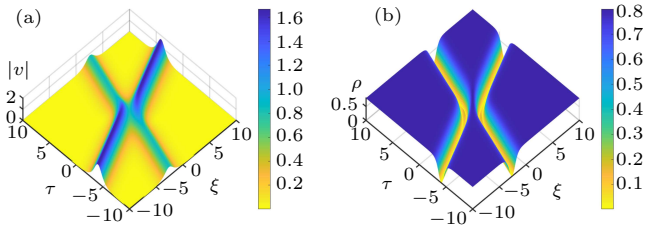


Fig. 2. Profiles of the solution $v^{[2]}$ (a) and $\rho^{[2]}$ (b) from Eq. (29) for the $(2+1)$-CCD system, under different parameter configurations: $\zeta_{1\mathrm{R}} = -\zeta_{1\mathrm{I}} = 0.3$, $\zeta_{2\mathrm{R}} = \zeta_{2\mathrm{I}} = 0.6$, $B_1 = -B_2 = -0.1$, and $B_3 = -B_4 = 0.2$, and $B_3 = -B_4 = 0.001$, and $a = -0.8$.

The solutions in Eq. (29) exhibit a range of dark and bright soliton profiles, shaped by the spectral parameters and the specific form of ν in Eqs. (A1)–(A3). When ν is linear, that is, $\nu = \xi + \eta + \tau$, the solutions correspond to standard bright and dark solitons. A quadratic form, $\nu = (\xi + \eta + \tau)^2$, results in parabolic profiles, while a sinusoidal form, $\nu = \sin(\xi + \eta + \tau)$, leads to periodic solutions. A cubic form, $\nu = (\xi + \eta + \tau)^3$, gives rise to S-shaped soliton structures. Figure 2 illustrates the interaction dynamics of two bright $v^{[2]}$ and two dark $\rho^{[2]}$ solitons in the (2+1)-CCD system. Bright solitons (Fig. 2(a)) exhibit localized peaks propagating with inherent acceleration, sustained by a balance of nonlinear focusing and dispersion. Meanwhile, dark solitons (Fig. 2(b)) appear as stable intensity dips on a background, maintained through phase-modulated interactions with their surroundings. These figures highlight soliton interactions influenced by parametric sensitivity: bright solitons emerge in regimes dominated by focusing nonlinearity, whereas dark solitons prevail under defocusing conditions.

Figures 3(a) and 4(a) highlight parabolic soliton structures in the $(2+1)$-CCD system. Figure 3(a) shows a bright parabolic soliton corresponding to the $v^{[2]}$ solution, characterized by a localized peak propagating in the ξ–τ plane. In contrast, figure 4(a) presents a dark parabolic soliton associated with solution $\rho^{[2]}$, distinguished by a localized dip. These visualizations reveal the distinct behaviors of bright and dark solitons, providing insight into the dynamics of the system and the impact of parameter variations.

Figures 3(b) and 4(b) depict the interaction of two periodic solitons in the $(2+1)$-CCD system. The solitons exhibit a repeating wave structure, maintaining their periodic nature as they propagate along the ξ- and τ-directions. The interaction region, visible at the center, shows a localized increase in wave intensity in Fig. 3(b), indicating constructive interference, while figure 4(b) shows a localized dip at the center. The periodic pattern remains intact after interaction, demonstrating a stable soliton collision where the wave profiles preserve their structure. This behavior highlights the integrability of the system, confirming the persistence of solitonic features even after nonlinear interactions.

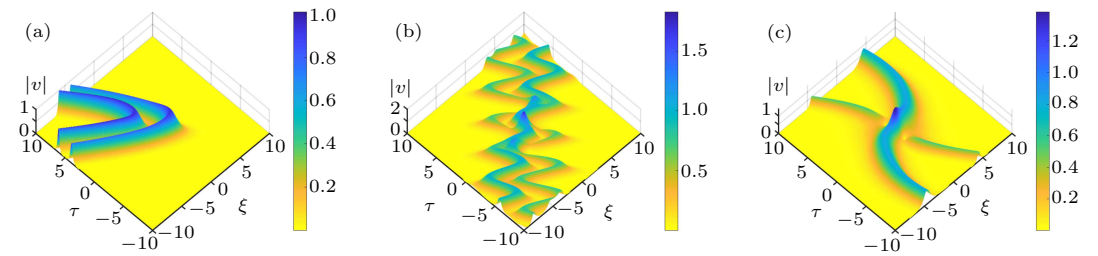


Fig. 3. Profiles of the solution $v^{[2]}$ from Eq. (29) for the $(2+1)$-CCD system, under different parameter configurations: (a) corresponds to $\zeta_{1\mathrm{R}} = -\zeta_{1\mathrm{I}} = 0.5$, $\zeta_{2\mathrm{R}} = \zeta_{2\mathrm{I}} = 0.6$, $B_1 = -B_2 = 1.2$, and $B_3 = -B_4 = 0.001$; (b) corresponds to $\zeta_{1\mathrm{R}} = \zeta_{1\mathrm{I}} = 0.5$, $\zeta_{2\mathrm{R}} = \zeta_{2\mathrm{I}} = 0.6$, $B_1 = -B_2 = 1.2$, and $B_3 = -B_4 = 1.5$; (c) corresponds to $\zeta_{1\mathrm{R}} = 0.8$, $\zeta_{1\mathrm{I}} = \zeta_{2\mathrm{I}} = 0.5$, $\zeta_{2\mathrm{R}} = 0.6$, $B_1 = -B_2 = 0.02$, and $B_3 = -B_4 = 0.001$, and $a = -0.8$.

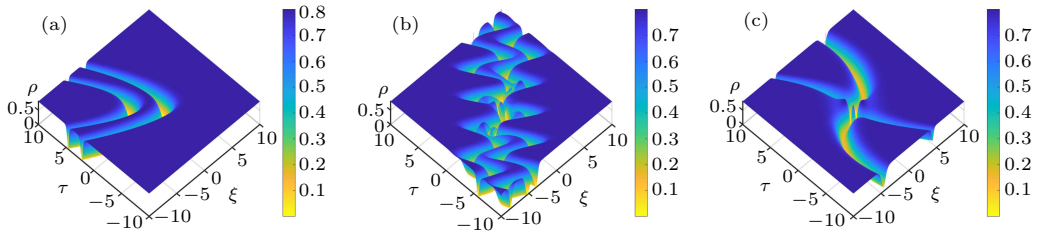


Fig. 4. The solution profiles of $\rho^{[2]}$ from Eq. (29) for the $(2+1)$-CCD system. These profiles are generated under different parameter settings, with all parameters kept the same as in Fig. 3, except for $B_1 = -B_2 = -0.1$ and $B_3 = -B_4 = 0.2$, corresponding to (a).

Figure 4(c) illustrates an S-shaped or cubic dark soliton in the $(2+1)$-dimensional CCD system. The soliton has a central dip, indicating a decrease in wave intensity, while figure 3(c) shows a central peak. The soliton extends outward in opposite directions, forming an S-like shape. The left and right parts propagate along the ξ-axis, while the upper and lower sections spread along the τ-axis. The central region represents the main interaction zone, where the wave undergoes significant changes. This structure arises because of specific system conditions, which demonstrate how solitons interact and evolve over time.

4. Conclusion

In this work, we have studied a (2+1)-CCD system and demonstrated its equivalence to the sine-Gordon equation and the negative flow of the modified Korteweg–de Vries hierarchy through suitable transformations. We constructed a Lax pair for this system, enabling the generation of multisoliton solutions using the Darboux transformation. These solutions, expressed as ratios of simple determinants, exhibit a wide range of structures, including bright and dark solitons, S-shaped formations, parabolic profiles, and periodic wave patterns.

Further exploration of this system could involve its generalization to an arbitrary nonabelian Lie group, where the Darboux transformation could be applied to derive broader classes of solutions. Furthermore, integrating machine learning techniques, such as physics-informed neural networks for unsupervised learning and Bayesian regularization backpropagation for supervised learning, could provide deeper insights into the system's behavior and facilitate the analysis of more complex scenarios. Another promising direction is the extension of the generalized (2+1)-dimensional complex coupled dispersionless system to more intricate configurations of current-fed strings in external magnetic fields, incorporating nonlocal effects. This would involve investigating the influence of varying magnetic field strengths, currents, boundary conditions, and external perturbations on wave dynamics, stability, and nonlinear interactions.

Future work will also focus on exploring the existence of rational solutions, such as lump solutions, for the equation studied. Identifying lump-type structures could provide valuable insights into the interplay between localized and nonlocal interactions. Furthermore, explicit solutions will be investigated by considering the seed solution $\rho = a$ and $v = c\,\mathrm{e}^{\mathrm{i}(\xi\kappa+\eta k+w\tau)}$. This approach is expected to lead to the discovery of breather and rogue wave solutions, which are of great interest in nonlinear wave phenomena.

Appendix A: Explicit expressions of ρ_{num}, v_{num}, and d_1

$$
\begin{aligned}
\rho_{\mathrm{num}} &= (\zeta_2-\zeta_1)(\zeta_3-\zeta_4)\\
&\times\Big(\zeta_3\zeta_4(\zeta_1+\zeta_2)\exp\Big(\frac{-2\mathrm{i}a\xi\,\zeta_1^2\zeta_2\zeta_3\zeta_4+(-2\mathrm{i}\xi\,\zeta_2^2\zeta_3\zeta_4a+(2\mathrm{i}\xi\,\zeta_3^2\zeta_4a+(2\mathrm{i}\zeta_4^2a\xi+2B_iv\zeta_4-\mathrm{i}\tau)\zeta_3-\mathrm{i}\zeta_4\tau)\zeta_2+\mathrm{i}\zeta_3\zeta_4\tau)\zeta_1+\mathrm{i}\tau\zeta_2\zeta_3\zeta_4}{2\zeta_1\zeta_4\zeta_3\zeta_2}\Big)\\
&+\zeta_2\zeta_1(\zeta_3+\zeta_4)\exp\Big(\frac{2\mathrm{i}a\xi\,\zeta_1^2\zeta_2\zeta_3\zeta_4+(2\mathrm{i}\xi\,\zeta_2^2\zeta_3\zeta_4a+(-2\mathrm{i}\xi\,\zeta_3^2\zeta_4a+(-2\mathrm{i}\zeta_4^2a\xi+2B_iv\zeta_4+\mathrm{i}\tau)\zeta_3+\mathrm{i}\zeta_4\tau)\zeta_2-\mathrm{i}\zeta_3\zeta_4\tau)\zeta_1-\mathrm{i}\tau\zeta_2\zeta_3\zeta_4}{2\zeta_1\zeta_4\zeta_3\zeta_2}\Big)\Big)\\
&+\zeta_2\zeta_4(\zeta_3-\zeta_1)(\zeta_1+\zeta_3)(\zeta_2-\zeta_4)\\
&\times\exp\Big(\frac{-2\mathrm{i}a\xi\,\zeta_1^2\zeta_2\zeta_3\zeta_4+(2\mathrm{i}\xi\,\zeta_2^2\zeta_3\zeta_4a+(-2\mathrm{i}\xi\,\zeta_3^2\zeta_4a+(2\mathrm{i}\zeta_4^2a\xi+4(B_2+B_4)v\zeta_4-\mathrm{i}\tau)\zeta_3+\mathrm{i}\zeta_4\tau)\zeta_2-\mathrm{i}\zeta_3\zeta_4\tau)\zeta_1+\mathrm{i}\tau\zeta_2\zeta_3\zeta_4}{2\zeta_1\zeta_4\zeta_3\zeta_2}\Big)\\
&+\zeta_2\zeta_3(\zeta_4-\zeta_1)(\zeta_1+\zeta_4)(\zeta_2-\zeta_3)\\
&\times\exp\Big(\frac{-2\mathrm{i}a\xi\,\zeta_1^2\zeta_2\zeta_3\zeta_4+(2\mathrm{i}\xi\,\zeta_2^2\zeta_3\zeta_4a+(2\mathrm{i}\xi\,\zeta_3^2\zeta_4a+(-2\mathrm{i}\zeta_4^2a\xi+4(B_2+B_3)v\zeta_4+\mathrm{i}\tau)\zeta_3-\mathrm{i}\zeta_4\tau)\zeta_2-\mathrm{i}\zeta_3\zeta_4\tau)\zeta_1+\mathrm{i}\tau\zeta_2\zeta_3\zeta_4}{2\zeta_1\zeta_4\zeta_3\zeta_2}\Big)\\
&+\zeta_1(\zeta_4(\zeta_2-\zeta_3)(\zeta_2+\zeta_3)(\zeta_4-\zeta_1)\\
&\times\exp\Big(\frac{2\mathrm{i}a\xi\,\zeta_1^2\zeta_2\zeta_3\zeta_4+(-2\mathrm{i}\xi\,\zeta_2^2\zeta_3\zeta_4a+(-2\mathrm{i}\xi\,\zeta_3^2\zeta_4a+(2\mathrm{i}\zeta_4^2a\xi+4(B_1+B_4)v\zeta_4-\mathrm{i}\tau)\zeta_3+\mathrm{i}\zeta_4\tau)\zeta_2+\mathrm{i}\zeta_3\zeta_4\tau)\zeta_1-\mathrm{i}\tau\zeta_2\zeta_3\zeta_4}{2\zeta_1\zeta_4\zeta_3\zeta_2}\Big)\\
&+\zeta_3\exp\Big(\frac{2\mathrm{i}a\xi\,\zeta_1^2\zeta_2\zeta_3\zeta_4+(-2\mathrm{i}\xi\,\zeta_2^2\zeta_3\zeta_4a+(2\mathrm{i}\xi\,\zeta_3^2\zeta_4a+(-2\mathrm{i}\zeta_4^2a\xi+4(B_1+B_3)v\zeta_4+\mathrm{i}\tau)\zeta_3-\mathrm{i}\zeta_4\tau)\zeta_2+\mathrm{i}\zeta_3\zeta_4\tau)\zeta_1-\mathrm{i}\tau\zeta_2\zeta_3\zeta_4}{2\zeta_1\zeta_4\zeta_3\zeta_2}\Big)\\
&\times(\zeta_2-\zeta_4)(\zeta_2+\zeta_4)(\zeta_3-\zeta_1)),
\end{aligned}
\tag{A1}
$$

$$
\begin{aligned}
v_{\text{num}} = & -\mathrm{i}(\zeta_3-\zeta_1)(\zeta_2-\zeta_3)\zeta_4^2(\zeta_2-\zeta_1)\\
& \times\exp\Big(\frac{-2\mathrm{i}a\xi\,\zeta_1^2\zeta_2\zeta_3\zeta_4+(-2\mathrm{i}\xi\,\zeta_2^2\zeta_3\zeta_4a+(-2\mathrm{i}\xi\,\zeta_3^2\zeta_4a+(2\mathrm{i}\zeta_4^2a\xi+2(B_2+B_1+2B_4)\nu\zeta_4-\mathrm{i}\tau)\zeta_3+\mathrm{i}\zeta_4\tau)\zeta_2+\mathrm{i}\zeta_3\zeta_4\tau)\zeta_1+\mathrm{i}\tau\zeta_2\zeta_3\zeta_4}{2\zeta_3\zeta_4\zeta_1\zeta_2}\Big)\\
& -\mathrm{i}(\zeta_2-\zeta_1)(\zeta_4-\zeta_1)\zeta_3^2(\zeta_2-\zeta_4)\\
& \times\exp\Big(\frac{-2\mathrm{i}a\xi\,\zeta_1^2\zeta_2\zeta_3\zeta_4+(-2\mathrm{i}\xi\,\zeta_2^2\zeta_3\zeta_4a+(2\mathrm{i}\xi\,\zeta_3^2\zeta_4a+(-2\mathrm{i}\zeta_4^2a\xi+2(B_2+B_1+2B_3)\nu\zeta_4+\mathrm{i}\tau)\zeta_3-\mathrm{i}\zeta_4\tau)\zeta_2+\mathrm{i}\zeta_3\zeta_4\tau)\zeta_1+\mathrm{i}\tau\zeta_2\zeta_3\zeta_4}{2\zeta_3\zeta_4\zeta_1\zeta_2}\Big)\\
& -\mathrm{i}(\zeta_2^2(\zeta_4-\zeta_1)(\zeta_3-\zeta_1)\\
& \times\exp\Big(\frac{-2\mathrm{i}a\xi\,\zeta_1^2\zeta_2\zeta_3\zeta_4+(2\mathrm{i}\xi\,\zeta_2^2\zeta_3\zeta_4a+(-2\mathrm{i}\xi\,\zeta_3^2\zeta_4a+(-2\mathrm{i}\zeta_4^2a\xi+2(2B_2+B_4+B_3)\nu\zeta_4+\mathrm{i}\tau)\zeta_3+\mathrm{i}\zeta_4\tau)\zeta_2-\mathrm{i}\zeta_3\zeta_4\tau)\zeta_1+\mathrm{i}\tau\zeta_2\zeta_3\zeta_4}{2\zeta_3\zeta_4\zeta_1\zeta_2}\Big)\\
& +\zeta_1^2\exp\Big(\frac{2\mathrm{i}a\xi\,\zeta_1^2\zeta_2\zeta_3\zeta_4+(-2\mathrm{i}\xi\,\zeta_2^2\zeta_3\zeta_4a+(-2\mathrm{i}\xi\,\zeta_3^2\zeta_4a+(-2\mathrm{i}\zeta_4^2a\xi+2(2B_1+B_4+B_3)\nu\zeta_4+\mathrm{i}\tau)\zeta_3+\mathrm{i}\zeta_4\tau)\zeta_2+\mathrm{i}\zeta_3\zeta_4\tau)\zeta_1-\mathrm{i}\tau\zeta_2\zeta_3\zeta_4}{2\zeta_3\zeta_4\zeta_1\zeta_2}\Big)\\
& \times(\zeta_2-\zeta_4)(\zeta_2-\zeta_3))(\zeta_3-\zeta_4),
\end{aligned}
\tag{A2}
$$

$$
\begin{aligned}
d_1 = & -\Big(\Big(\exp\Big(\frac{-2\mathrm{i}a\xi\,\zeta_1^2\zeta_2\zeta_3\zeta_4+(-2\mathrm{i}\xi\,\zeta_2^2\zeta_3\zeta_4a+(2\mathrm{i}\xi\,\zeta_3^2\zeta_4a+(2\mathrm{i}\zeta_4^2a\xi+2B_i\nu\zeta_4-\mathrm{i}\tau)\zeta_3-\mathrm{i}\zeta_4\tau)\zeta_2+\mathrm{i}\zeta_3\zeta_4\tau)\zeta_1+\mathrm{i}\tau\zeta_2\zeta_3\zeta_4}{2\zeta_1\zeta_4\zeta_3\zeta_2}\Big)\\
& +\exp\Big(\frac{2\mathrm{i}a\xi\,\zeta_1^2\zeta_2\zeta_3\zeta_4+(2\mathrm{i}\xi\,\zeta_2^2\zeta_3\zeta_4a+(-2\mathrm{i}\xi\,\zeta_3^2\zeta_4a+(-2\mathrm{i}\zeta_4^2a\xi+2B_i\nu\zeta_4+\mathrm{i}\tau)\zeta_3+\mathrm{i}\zeta_4\tau)\zeta_2-\mathrm{i}\zeta_3\zeta_4\tau)\zeta_1-\mathrm{i}\tau\zeta_2\zeta_3\zeta_4}{2\zeta_1\zeta_4\zeta_3\zeta_2}\Big)\Big)(\zeta_3-\zeta_4)(\zeta_2-\zeta_1)\\
& +(\zeta_3-\zeta_1)\Big(\exp\Big(\frac{-2\mathrm{i}a\xi\,\zeta_1^2\zeta_2\zeta_3\zeta_4+(2\mathrm{i}\xi\,\zeta_2^2\zeta_3\zeta_4a+(-2\mathrm{i}\xi\,\zeta_3^2\zeta_4a+(2\mathrm{i}\zeta_4^2a\xi+4(B_2+B_4)\nu\zeta_4-\mathrm{i}\tau)\zeta_3+\mathrm{i}\zeta_4\tau)\zeta_2-\mathrm{i}\zeta_3\zeta_4\tau)\zeta_1+\mathrm{i}\tau\zeta_2\zeta_3\zeta_4}{2\zeta_1\zeta_4\zeta_3\zeta_2}\Big)\\
& +\exp\Big(\frac{2\mathrm{i}a\xi\,\zeta_1^2\zeta_2\zeta_3\zeta_4+(-2\mathrm{i}\xi\,\zeta_2^2\zeta_3\zeta_4a+(2\mathrm{i}\xi\,\zeta_3^2\zeta_4a+(-2\mathrm{i}\zeta_4^2a\xi+4(B_1+B_3)\nu\zeta_4+\mathrm{i}\tau)\zeta_3-\mathrm{i}\zeta_4\tau)\zeta_2+\mathrm{i}\zeta_3\zeta_4\tau)\zeta_1-\mathrm{i}\tau\zeta_2\zeta_3\zeta_4}{2\zeta_1\zeta_4\zeta_3\zeta_2}\Big)\Big)(\zeta_2-\zeta_4)\\
& +(\zeta_2-\zeta_3)\exp\Big(\frac{-2\mathrm{i}a\xi\,\zeta_1^2\zeta_2\zeta_3\zeta_4+(2\mathrm{i}\xi\,\zeta_2^2\zeta_3\zeta_4a+(2\mathrm{i}\xi\,\zeta_3^2\zeta_4a+(-2\mathrm{i}\zeta_4^2a\xi+4(B_2+B_3)\nu\zeta_4+\mathrm{i}\tau)\zeta_3-\mathrm{i}\zeta_4\tau)\zeta_2-\mathrm{i}\zeta_3\zeta_4\tau)\zeta_1+\mathrm{i}\tau\zeta_2\zeta_3\zeta_4}{2\zeta_1\zeta_4\zeta_3\zeta_2}\Big)\\
& +\Big(\exp\Big(\frac{2\mathrm{i}a\xi\,\zeta_1^2\zeta_2\zeta_3\zeta_4+(-2\mathrm{i}\xi\,\zeta_2^2\zeta_3\zeta_4a+(-2\mathrm{i}\xi\,\zeta_3^2\zeta_4a+(2\mathrm{i}\zeta_4^2a\xi+4(B_1+B_4)\nu\zeta_4-\mathrm{i}\tau)\zeta_3+\mathrm{i}\zeta_4\tau)\zeta_2+\mathrm{i}\zeta_3\zeta_4\tau)\zeta_1-\mathrm{i}\tau\zeta_2\zeta_3\zeta_4}{2\zeta_1\zeta_4\zeta_3\zeta_2}\Big)\Big)(\zeta_4-\zeta_1)\Big)\\
& \times\zeta_3\zeta_1\zeta_2\zeta_4,
\end{aligned}
\tag{A3}
$$

where $B_i = B_1+B_2+B_3+B_4$.

References

[1] Kivshar Y S and Agrawal G P 2003 *Optical solitons: from fibers to photonic crystals* (Academic Press)

[2] Malomed B A 2014 *The Sine-Gordon Model and Its Applications: From Pendula and Josephson Junctions to Gravity and High-Energy Physics* 1–30

[3] Ablowitz M J and Clarkson P A 1991 *Solitons, nonlinear evolution equations and inverse scattering*, Vol. 149 (Cambridge University Press)

[4] Wang D S, Zhu C and Zhu X 2025 *J. Differ. Equ.* **416** 642

[5] Zhang G and Yan Z 2020 *Physica D* **402** 132170

[6] Ma X and Zhu J 2023 *Stud. Appl. Math.* **151** 676

[7] Liu S, Tian B and Wang M 2021 *Eur. Phys. J. Plus* **136** 1

[8] Xu G q 2019 *Appl. Math. Lett.* **97** 81

[9] Konno K and Wadati M 1975 *Prog. Theor. Phys.* **53** 1652

[10] Gao X Y, Guo Y J and Shan W R 2022 *Chaos, Solitons and Fractals* **162** 112486

[11] Xie W K and Fan F C 2023 *J. Math. Anal. Appl.* **525** 127251

[12] Belokolos E D, Bobenko A I, Enolskii V Z, Its A R and Matveev V B 1994 *Algebro-geometric approach to nonlinear integrable equations*, Vol. 550 (Springer-Verlag)

[13] Moretlo T, Adem A R and Muatjetjeja B 2022 *Commun. Nonlinear Sci. Numer. Simul.* **106** 106072

[14] Yao Y, Yi H, Zhang X and Ma G 2023 *Chin. Phys. Lett.* **40** 100503

[15] Shao H and Sudao B 2023 *Chin. Phys. B* **32** 050204

[16] Matveev V B and Salle M A 1991 *Darboux Transformations and Solitons* (Springer Berlin Heidelberg)

[17] Riaz H W A, Lin J and Wang J 2024 *Phys. Lett. A* **528** 130060

[18] Riaz H W A and Lin J 2024 *Appl. Math. Lett.* **158** 109217

[19] Wen X Y, Lin Z and Wang D S 2024 *Phys. Rev. E* **109** 044215

[20] Takasaki K and Takebe T 1995 *Rev. Math. Phys.* **7** 743

[21] Calderbank D M and Kruglikov B 2021 *Commun. Math. Phys.* **382** 1811

[22] Konno K and Oono H 1994 *J. Phys. Soc. Jpn.* **63** 377

[23] Kakuhata H and Konno K 1996 *J. Phys. Soc. Jpn.* **65** 340

[24] Kakuhata H and Konno K 1999 *J. Phys. Soc. Jpn.* **68** 757

[25] Kotlyarov V P 1994 *J. Phys. Soc. Jpn.* **63** 3535

[26] Shen S, Feng B F and Ohta Y 2016 *Stud. Appl. Math.* **136** 64

[27] Riaz H W A and ul Hassan M 2018 *J. Math. Anal. Appl.* **458** 1639

[28] Eren K and Ersoy S 2023 *Complex Var. Elliptic Equ.* **68** 1984

[29] Wang G, Yang K, Gu H, Guan F and Kara A 2020 *Nucl. Phys. B* **953** 114956

[30] Anco S C and Wolf T 2005 *J. Nonllinear Math. Phys.* **12** 13

[31] Gelfand I, Gelfand S, Retakh V and Wilson R L 2005 *Adv. Math.* **193** 56

[32] Pogrebkov A K 2014 *Theor. Math. Phys.* **181** 1585